Phonon spectroscopy of superconducting Nb using point-contact tunneling

Qiang Huang,* J. F. Zasadzinski,* and K. E. Gray
Materials Science Division, Argonne National Laboratory, Argonne, Illinois 60439
(Received 9 April 1990)

Tunneling spectroscopy measurements have been made on single crystals of Nb using the point-contact technique with a Au tip. The current-voltage characteristics, $I(V)$ and dI/dV, reproduce the results obtained from conventional, thin-film planar junctions. In the range of 5- to 50-meV bias, the tunneling conductance displays the characteristic structures associated with the phonon density of states for Nb, including a low-energy mode near 10 meV, previously observed only in junctions on the (100) crystal face. These results demonstrate that the point-contact tunneling method can be used to measure the electron-phonon interaction in superconductors with the same degree of sensitivity as found in thin-film tunneling spectroscopy. The high-bias conductance was always an increasing function of voltage, as expected for tunnel-barrier transmission, and never displayed the anomalous decreasing behavior found in low-resistance junctions on high-temperature superconductors (HTS's). We draw some inferences about the effects of heating and discuss them in relation to point-contact tunneling into the HTS materials.

I. INTRODUCTION

The method of electron-tunneling spectroscopy on macroscopic junctions has been responsible for a number of fundamental observations including a detailed picture of the electron-phonon interaction in superconductors.[1] Conventional (macroscopic) junctions are typically formed in a planar geometry by using a thin metal film for one or both electrodes, but this "thin-film" method has several limitations, including spatial averaging of properties over the junction area, potential influence of surface oxides on the tunneling measurement, and the incompatibility with small specimens such as single crystals. We present the first demonstration of a quantitative measurement of the electron-phonon interaction in a moderately coupled superconductor using point-contact tunneling. The technique of forming a junction by mechanically bringing the pointed tip of an electrode near the surface of a specimen is emerging as a powerful spatial and spectroscopic probe. For example, the scanning tunneling microscope (STM) has evolved into a sophisticated tool for direct imaging of many surfaces with atomic resolution.[2]

The STM maintains a separation between the tip and sample resulting in high tunneling resistances (10^7-10^9 Ω), and a relatively poor signal-to-noise ratio compared to thin-film junctions. Nevertheless, measurements of the current-voltage characteristics, $I(V)$, and the dynamic conductance, $\sigma=dI/dV$, have been performed which unambiguously show the energy gap of superconductors[3] and structure[4] from the phonon density of states (DOS) of Pb. Relatively large changes in conductance take place near the gap energy ($eV=\Delta$) of a superconductor and by incorporating signal-averaging techniques, a reasonably well-defined BCS DOS can be obtained[3] with a STM. Similarly, the conductance deviations near the phonon peak energies in Pb junctions, which are quite large (nearly 10%), can be observed in the STM dI/dV spectra.[4] The powerful combination of spatial and spectral resolution in a STM has recently been demonstrated in the mapping of the Abrikosov flux lattice and electronic structure of the vortex cores[5] in superconducting $NbSe_2$. Lower junction resistances (10^3-10^5 Ω) are usually interpreted as the STM tip actually touching the sample surface and, in such a point-contact geometry, an insulating surface layer serves as the tunnel barrier.

Despite the advances of the STM and point-contact method for performing local spectroscopy, the question remains whether these techniques are capable of the high-resolution phonon spectroscopy found in thin-film junctions which is necessary for a quantitative determination of the electron-phonon interaction in superconductors, namely, the Eliashberg function $\alpha^2F(\omega)$. Here, $F(\omega)$ is the phonon DOS and α^2 is a measure of the coupling strength of the electrons to phonons of frequency ω. To date, no phonon structure has been reported for any moderately coupled superconductor such as Nb ($\lambda=1.0$), by either STM or point-contact tunneling. Such tests of point-contact tunneling are a prerequisite to the search for phonons or other pairing mechanisms in high-temperature superconductors (HTS) by this method.

With only a few exceptions, point-contact tunneling has been necessary[6] for tunneling in HTS, since they can exhibit thick insulating surface layers and the tip can be used to mechanically scrape, clean, or even cleave the sample surface. There exists a large variation in the reported HTS energy gaps measured by point-contact tunneling, although most of this can be attributed to charging effects,[6-8] gap anisotropy, and/or poor surfaces. Also, the search for phonon structure in the dI/dV has been obscured by other structures which appear to be from additional conduction channels (e.g., inelastic tunneling[9] or conduction through the barrier). There is speculation that the narrow tip can lead to heating and/or depairing effects from the high current density. Considering the nonideal tunneling characteristics ob-

served in HTS, it is important to determining whether any of these are inherent to the point-contact method.

We report here high-resolution tunneling spectroscopy measurement on single-crystal Nb using a point-contact apparatus described earlier[10] and recently used for tunneling studies on single crystals of $^{11}Bi_{1.7}Pb_{0.3}Sr_2CaCu_2O_x$ (Bi-Pb-Sr-Ca-Cu-O) and[12] $Tl_2Ba_2CaCu_2O_x$ (Tl-Ba-Ca-Cu-O). Niobium has been studied extensively by conventional and proximity-effect tunneling methods[13–15] so its phonon spectrum is well established. Also, the phonon structures in Nb junctions are rather small, about a 1% change in dI/dV, and therefore present a challenging test for the point-contact method. We find ideal, low-leakage $I(V)$ characteristics and a tunneling conductance which always increases with bias voltage, as is typical of barrier transmission. The superconducting conductance spectra reproduce the phonon structure found in conventional junctions on the (100) face of single-crystal Nb. The strength of the structure, as given by the deviation of the tunneling density of states from the BCS value, is comparable to previous work[13–15] ($\sim$1%), and indicates that there are no apparent effects from the point-contact geometry which either depress the superconductivity near the tip or dampen the subtle phonon structure. These results represent the first demonstration that the point-contact tunneling method can have sufficient precision to determine quantitatively the electron-phonon interaction in a superconductor.

II. EXPERIMENTAL METHODS AND RESULTS

The Nb single crystals were prepared by the resistive heating of high-purity foils near the melting point for about 24 h in a vacuum of low 10^{-9} torr. The final anneal locally melts the foil, abruptly cutting off the current, and near the region of melting we find single crystals about 1 mm^2 or larger in area. After etching one of the crystals in acid, it was mounted to the tunneling apparatus and placed in a vacuum can. The particular crystal used was close to the melted region in the center of the foil and such crystals were found to display a surface normal in the [100] direction.[16] Low-temperature measurements were always done by cooling with exchange gas to liquid ^{4}He (2–5 K) or liquid N_2 (77 K).

As in cases with HTS crystals, the Au tip was used to mechanically scrape the surface and this procedure allowed us to obtain both low-resistance (5–10 Ω), superconductor-normal (SN), pure-metallic contacts and tunneling contacts with junction resistances $R_N \sim 0.4$–20 kΩ, by adjusting the tip position. The point-contact tunnel junctions were clearly identified by the $I(V)$ which displayed low-leakage currents and a well-defined Nb energy gap. An example is shown in Fig. 1 for junction 1 with $R_N = 3.5$ kΩ: the contribution to the leakage current from nontunneling processes is less than 5%. For some junctions, leakage currents below 1% were observed.

The superconducting gap parameter Δ was determined by two methods. By plotting V^2 versus I^2, the V^2 intercept gives $(\Delta/e)^2$ directly for a BCS superconductor.

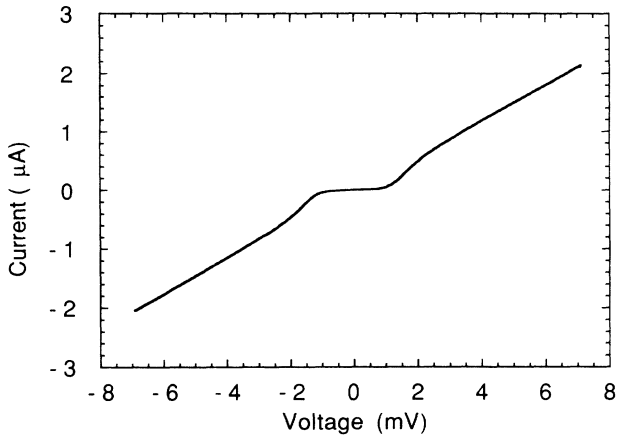

FIG. 1. Current-voltage characteristic $I(V)$ for junction 1, showing the typical low-leakage current (<5%). Energy gap parameter obtained from this curve is $\Delta = 1.50 \pm 0.02$ meV.

Another procedure used was to fit the normalized tunneling conductance directly with the calculated BCS DOS which was smeared to account for finite-temperature effects. Both methods gave similar values and, for the junction in Fig. 1, $\Delta = 1.50 \pm 0.02$ meV for $T = 2$ K. This value compares favorably with previous work using conventional and proximity-effect junctions, although it is slightly smaller than the 1.54 meV (at $T = 1.5$ K) reported for ideal conventional junctions,[14] i.e., those formed without any exposure of the Nb surface to oxygen. The slightly reduced value we obtain is presumably due to a thin proximity layer between the Nb and the insulating oxide which is well known to occur in air-oxidized junctions.[13]

Dynamics conductance measurements were obtained using a bridge circuit and standard harmonic detection methods. The superconducting conductance (σ_S) for junction 1 is shown in Fig. 2 as solid circles, while the solid line is smoothed σ_S and the dashed line is the

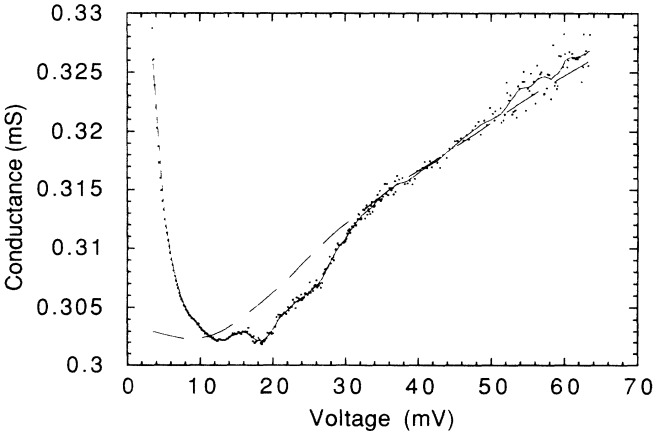

FIG. 2. Dynamic conductance dI/dV data for junction 1. The superconducing data are shown as solid circles, the smoothed superconducting curve (σ_S) is shown as the solid line, and the smoothed normal-state curve (σ_N) is shown as the dashed line.

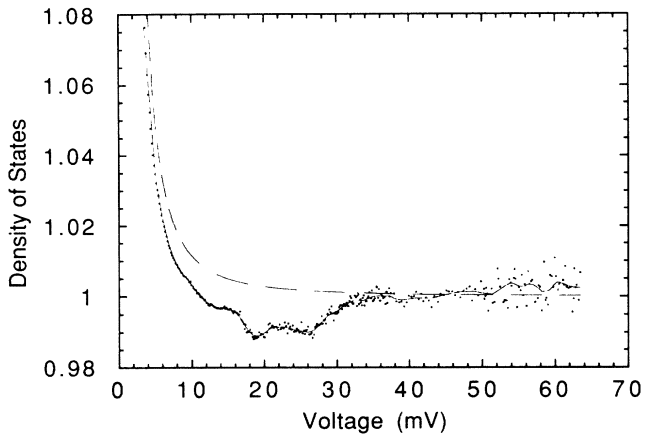

FIG. 3. Comparison of the tunneling density of states (DOS) $\sigma=\sigma_S/\sigma_N$ to the BCS DOS σ_{BCS}. The tunneling DOS data are shown as solid circles, the smoothed tunneling data are shown as the solid line, and the BCS DOS is shown as the dashed line. The Nb phonon structures near 17 and 25 mV are clearly seen as deviations from the BCS DOS.

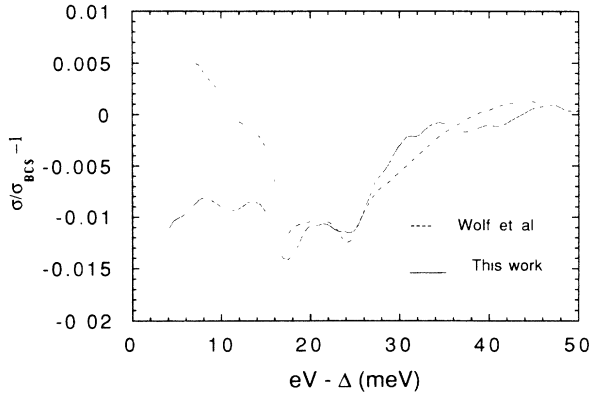

FIG. 4. Comparison of the reduced DOS $\sigma/\sigma_{BCS}-1$ for junction 1 of this study and the data of Wolf *et al.* (Ref. 16) using thin-film junctions on the (100) face of Nb. The energy scale is plotted from the gap edge. The overall agreement in the location and strength of the phonon structures is good. We note that subtle structure is seen near 10 meV in both junctions.

smoothed σ_N. The smooth curves used a least-squares, polynomial fitting procedure. The structures near 18 and 27 meV in Fig. 2 are the characteristic deviations[13–15] of the tunneling conductance due to peaks in the phonon DOS of Nb. To obtain a measure of the strength of this structure, we compute the normalized conductance $\sigma=\sigma_S/\sigma_N$, which is the experimental tunneling DOS, $N_T(E)$, and compare this to a BCS DOS, σ_{BCS}, in Fig. 3. The observation of phonon effects is due to the energy dependence of the pair potential $\Delta(E)$ which affects the measured tunneling density of states

$$N_T(E)=\mathrm{Re}\{E/[E^2-\Delta^2(E)]^{1/2}\} .$$

We note that the phonon structure represents a deviation of conductance of only about 1% from the BCS curve, thus emphasizing the severe constraint on the allowable noise level. In this experiment, the noise can be estimated by the spread of data about the smoothed curve in Fig. 3. In the region 5–35 meV, the noise level is sufficiently less than the structure to give confidence that the structures are due to phonon effects. Above 50 meV, the noise level increases and the fluctuations about the smoothed curve are too large to give statistical significance to the structure. For this reason we focus our further analysis on the data up to 50 meV, which is well above the cutoff in the phonon spectrum of Nb.

The quantity that ultimately determines the Eliashberg function $\alpha^2F(\omega)$ is the reduced conductance $\sigma/\sigma_{BCS}-1$, which is generally plotted versus energy from the gap edge (eV $-\Delta$): in Fig. 4, we compare our result to that of Wolf *et al.*[16] for thin-film junctions on similarly prepared Nb foils. There is good agreement on the location of the phonon structures and there are comparable strengths of the longitudinal mode at 25 meV and transverse mode near 17 meV. While both curves indicate a pronounced phonon peak near 10 meV, our results display a continued negative deviation from BCS in this region. One possible explanation is that the normal-state conductance, taken at $T>T_c$, is slightly different from the background conductance of the superconducting data (taken at $T=2.0$ K), resulting in an incomplete factoring out of the background conductance. In the work of Wolf *et al.*,[16] the normal-state conductance is obtained by applying a magnetic field above H_{c2} while keeping T fixed.

The phonon structure at 10 meV has previously been observed only for junctions on the (100) face of Nb and it has been shown that this gives rise to an enhancement of $\alpha^2F(\omega)$ at 10 meV compared to the (110) face.[16] Our results confirm the presence of a 10-meV phonon and, while we have not measured the structural orientation of our crystal, the junction is most likely on the (100) face, based on previous measurements of such foils.[16] This comparison of (100) and (110) tunneling has been presented by Wolf *et al.*[16] as evidence for gap anisotropy in Nb. Another study comparing the tunneling spectra formed on (110) and (111) faces also suggested gap anisotropy.[17]

Details of the low-energy phonon structure can be found in the second-harmonic data d^2V/dI^2 shown in Fig. 5. Dips in the second-harmonic data correspond directly to peaks in the phonon DOS. Again we compare our results to those of Wolf *et al.*[16] and, while the overall shapes of the curves are similar, we note that the point-contact data show a more sharply resolved phonon structure near 10 meV and an additional dip near 7 meV, which is also observed in other junctions. The high-energy phonon peaks appear to be broader in the point-contact junctions compared to the thin-film junctions. It is not clear at the present time whether these small discrepancies are due to systematic differences in the tunneling measurements or whether the gap anisotropy is playing a role. Observation of anisotropy through the wave-vector or **k**-dependent Eliashberg function $\alpha^2(\mathbf{k},\omega)F(\mathbf{k},\omega)$ is possible because tunneling electrons are oriented primarily normal to the tunnel barrier and therefore have **k** within a narrow cone centered at $\mathbf{k}_\perp$. The particular **k** vectors within this cone are approximately normal to the crystal face, in this case (100). Perhaps the confined geometry of the point-contact re-

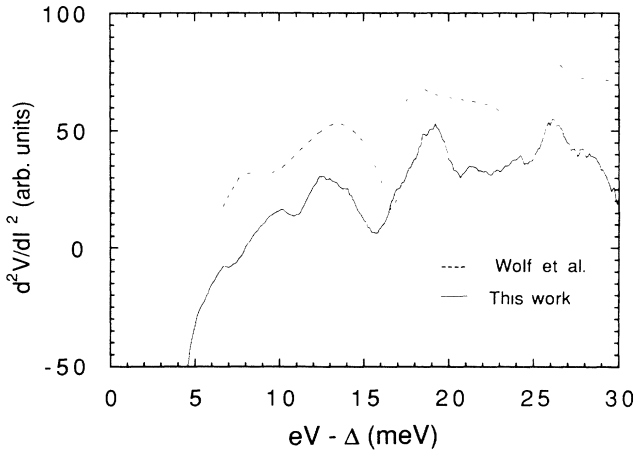

FIG. 5. Comparison of the second-harmonic tunneling data d^2V/dI^2 for junction 1 of this study and that of Wolf *et al.* (Ref. 16). While the agreement in location of the phonon structures is good, the point-contact data are broader for the *TA* mode near 16 meV but sharper for the mode near 10 meV and indicate an additional feature near 7 meV.

sults in a slightly different selection of **k** vectors compared to the larger area, thin-film junctions.

Point-contact junctions made in different regions of the single crystal, but still on the same face, showed similar results. In Fig. 6, both dI/dV and d^2I/dV^2 are shown for junction 2 in the superconducting state. In this case, the second-derivative data has been generated numerically from the tunneling conductance which accounts for the jagged features compared to the direct measurement of Fig. 5. We display both positive- and negative-bias voltages to show the symmetry of the phonon structure and to give a sense of the background conductance. It should be noted that phonon structure is antisymmetric in the second derivative such that for positive (negative) bias, dips (peaks) in d^2V/dI^2 correspond to peaks in $F(\omega)$. The phonon effects are similar to those of Figs. 4

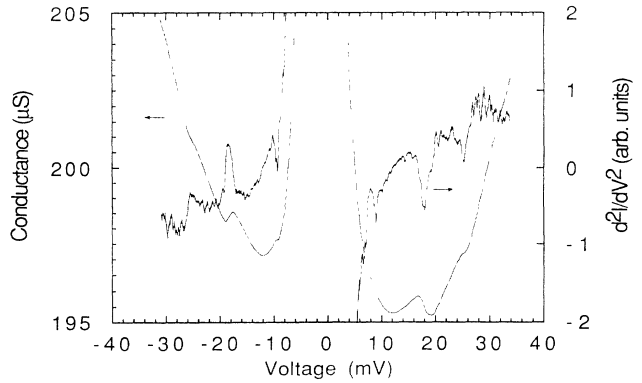

FIG. 6. Dynamic conductance dI/dV and d^2I/dV^2 for junction 2 in the superconducting state. The second derivative data were generated numerically from the dI/dV data which accounts for the jagged features compared to the measurements shown in Fig. 5. The phonon features of junction 1 are reproduced in junction 2, including the structure near 10 mV. The background tunneling conductance can be inferred from the superconducting dI/dV and indicates roughly parabolic behavior.

and 5: in particular, the low-energy structures at 8 and 11 meV (Δ not subtracted) are clearly evident in both curves. By comparing the dI/dV of Fig. 6 with the normal-state curve of Fig. 2, we infer a background tunneling conductance which is roughly parabolic in shape. A parabolic, increasing function of bias is expected for barrier transmission when the bias voltage is small compared to the barrier height[18] and the shape of the data is consistent with our initial assumption that the tunnel barrier is due to the oxidized surface of the Nb crystal, principally Nb_2O_5. The sharply increasing background conductance is typical of Nb oxide[19] and is due to the relatively low barrier height ϕ of $\sim$250 meV.

There are two important conclusions from this point-contact tunneling data when compared to conventional Nb thin-film junctions: phonon effects can be observed with the same excellent resolution; and there are no examples of obvious anomalous effects in the point-contact tunneling conductance.

III. HEATING EFFECTS AND IMPLICATIONS TO POINT-CONTACT TUNNELING IN HIGH-TEMPERATURE SUPERCONDUCTORS

In previous point-contact tunneling investigations of[11] Bi-Pb-Sr-Ca-C-O and[12] Tl-Ba-Ca-Cu-O single crystals, a systematic change of the background conductance was observed from increasing-with-bias to decreasing-with-bias as the overall junction resistance R_N decreased. It was concluded that the decreasing background conductance might be due to a narrow electron DOS, $N_n(E)$, centered approximately at the Fermi energy E_F. Although heating or current-depairing effects could occur in the superconductor locally near the tip of the point-contact electrode, thus decreasing the background conductance, it was argued that such localized, normal regions were inconsistent with our data.[11] In the following we discuss the potential effects of heating on similar point-contact tunneling measurements presented above for Nb.

Heating effects will be the largest for high-conductance junctions at large voltages. Examples of relatively low- and high-conductance junctions are shown in Fig. 7. The background conductance is given by the superconducting data for $eV \gg \Delta$. In the low-resistance junction of Fig. 7(a) σ is a slowly increasing function of voltage, changing over the entire voltage range by only about 20%. The shape of σ changes from parabolic at low voltages to roughly linear dependence at high voltages. All low-resistance ($R_N < 1$ kΩ) point-contact junctions had such a relatively flat background, in contrast to the high-resistance junctions which exhibited a much stronger dependence on bias voltage, as shown in Fig. 7(b) where the overall change in σ is about 100% out to 200 mV. The question is whether heating is responsible for the flatter σ versus V data found in the lower R_N junction. A heating model for a pure-metallic contact[20] has convincingly explained point-contact measurements in UPt_3. In this model, heat is dissipated by resistance processes in the metals, and it is therefore inappropriate to tunnel junctions where the heat is dissipated locally at the junc-

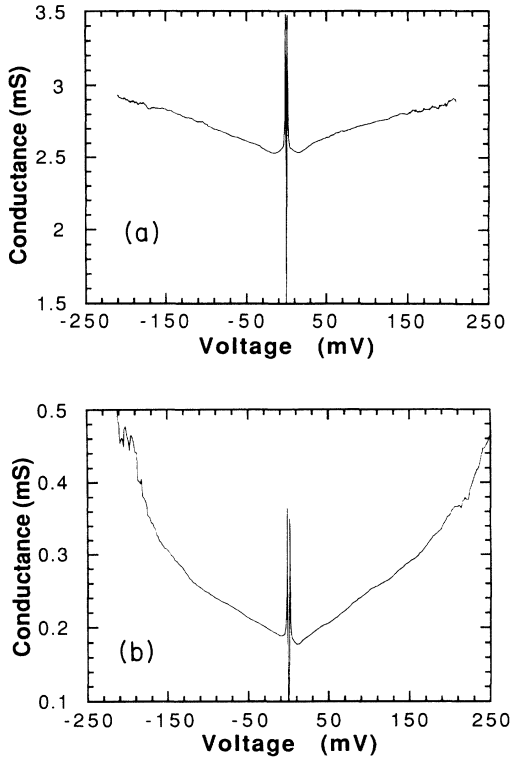

FIG. 7. The high-bias tunneling conductance dI/dV for (a) a low-resistance ($\sim 400\ \Omega$) junction and (b) a high-resistance (~ 5 kΩ) junction. The high-resistance junction displays a sharply increasing background conductance whereas the low-resistance junction has a weak voltage dependence.

tion. The Nb data presented here clearly arises from tunneling, rather than pure metallic contacts, since the conductance closely follows the BCS DOS at low voltage.

The simplest appropriately modified model for tunnel junctions assumes a disklike, circular point-contact junction of radius r_0. As the heat diffuses away from the junction, it expands either into a infinite half-space, or into cone of half-angle θ for the Au tip. The heat-flow equation becomes

$$\int_{T_j}^{T_b} \kappa(T)dT = \int_0^{\infty} \frac{VIdx}{A(x)} , \tag{1}$$

where T_j is the junction (maximum) temperature, T_b is the bath temperature, $\kappa(T)$ is the thermal conductivity, and $A(x)$ is the area. A convenient expression which incorporates the limits of large and small x/r_0 correctly is

$$A(x) = \pi[r_0^2 + 2x^2(1-\cos\theta)] .$$

Then Eq. (1) becomes

$$\int_{T_j}^{T_b} \kappa(T)dT = -\frac{VI}{2r_0\sqrt{2(1-\cos\theta)}} . \tag{2}$$

Now consider the case in which all the heat flows out the high-conductivity Au tip in which $\kappa(T) = sT$. Then Eq. (2) is easily solved to give

$$T_j^2 = T_b^2 + \frac{V^2/R_N}{sr_0\sqrt{2(1-\cos\theta)}} , \tag{3}$$

where $R_N = V/I$.

Experimentally, it is clear from the low-voltage data presented in Figs. 2–6 that heating is a negligible effect for 3.5–5 kΩ junctions. Any temperature increase at the junction must be a small fraction of $T_c - T_b$, where T_b is the bath temperature of ~ 2 K and $T_c = 9.2$ K, or else the decreased energy gap would reduce the phonon structure as Δ^2. The appearance of the full phonon structure at 20–35 mV implies that $\Delta(T_j) \sim \Delta(0)$ and therefore $T_j - T_b \ll T_c - T_b$, and the data sets a lower limit on the actual junction radius r_0. Assuming $T_j < 4$ K, $\theta = 20°$ and a conservative estimate for s of 0.1 W/cm K^2, we find r_0 must be greater than ~ 8 nm, which is quite acceptable.

At voltages above the maximum phonon frequency ($V > 35$ mV), we know on firm theoretical and experimental grounds that there are no definitive differences between the superconducting and normal-state conductances to test whether a significant temperature increase occurs. Thus, we can make no direct conclusion as to whether heating above T_c has occurred for $V > 35$ mV. Nonetheless, heating of the Nb above T_c would result in an extra resistance in series with the junction and a consequent decrease in the measured σ. However, the normal-state resistivity ρ_n of Nb is so small that such a contribution will be negligible [$< 0.1\ \Omega$ using ρ_n (10 K) $= 0.1\ \mu\Omega$ cm] even for the smallest $r_0 = 8$ nm from above. Even at room temperature, the contribution would be less than 7 Ω. Thus, differences in Fig. 7 for the shapes of σ at large voltages are *almost certainly not due to heating effects.*

The above model for heating can be applied to the HTS measurements in[11] Bi-Pb-Sr-Ca-Cu-O and[12] Tl-Ba-Ca-Cu-O since, in both cases, the conductance approximates the BCS DOS far better than that of a pure-metallic contact and therefore tunneling clearly dominates. If all the tunneling dissipation flows out the Au tip, Eq. (3) predicts the junction temperature can exceed $T_c \sim 100$ K at $V = 100$ mV and $R_N = 1000\ \Omega$ only if $r_0 < 0.2$ nm. A second scenario is that the power dissipated in the HTS (half of the total) is forced to flow out through the HTS rather than the Au tip: this requires a significant thermal boundary resistance at the junction which is unlikely considering the large pressure between the small-area Au tip and the HTS crystal and such higher temperatures (~ 100 K). Nevertheless, if we use a conservative estimate of the thermal conductivity of 0.01 W/cm K from measurements[21] on $YBa_2Cu_3O_y$ and assumed the HTS occupies the infinite half-space ($\theta = 90°$), then Eq. (3) predicts the junction can exceed $T_c \sim 100$ K for $V = 100$ mV and $R_N = 1000\ \Omega$ only if $r_0 < 30$ nm. Although the analysis does not favor significant heating effects in the HTS point-contact junctions, we do not know the junction areas, so no definitive conclusion can be drawn. The potential role of anisotropy in the thermal conductivity of the HTS is harder to estimate, but over large distance scales that anisotropy is measured[21] it is relatively small (~ 5).

The absence of heating effects leads us to analyze the Nb data of Fig. 7 using a tunneling model.[18] Assuming a rectangular barrier of height ϕ, this model leads to a parabolic dependence of $\sigma(V)$ for $V \ll \phi$. While the data of

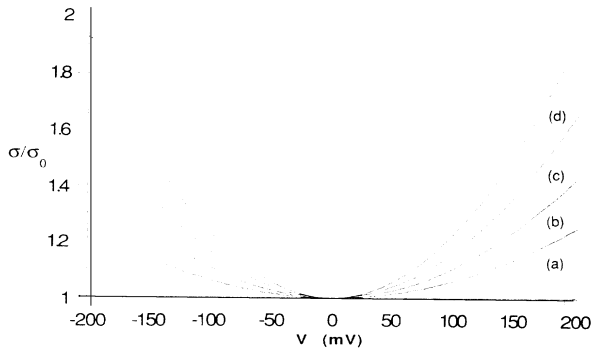

FIG. 8. The calculated tunneling conductances for a junction fixed area (contact radius $r_0=130$ nm) barrier height of 250 meV and barrier thickness [from (a) through (d)] of 1, 1.2, 1.4, and 1.6 nm. These result in $R_N=0.2$, 0.67, 2.2, and 6.9 kΩ, respectively, which are within the measured range.

Fig. 7 do not display a simple parabolic shape, we expect the model to give a reasonable approximation to the background conductance, and more importantly, to show the systematic change of the background shape with junction resistance. The results of modeling tunnel junctions with a rectangular barrier of various thicknesses and $\phi=250$ meV are shown in Fig. 8, in which the tunneling conductance σ is normalized to the zero-bias value σ_0 for clarity. We choose to interpret different zero-bias resistances as being due primarily to differences in barrier thickness rather than junction area: this is because the shapes of the measured σ at large voltages varied with R_N in a consistent manner, which would not be the case if the junction area was changing significantly.

If the junction area is fixed at a reasonable value (contact radius, $r_0=130$ nm), then barrier thicknesses of 1, 1.2, 1.4, and 1.6 nm result in $R_N=0.2$, 0.67, 2.2, and 6.9 kΩ, respectively, which are within the measured range in Fig. 7. For that range of R_N, the increase in conductance out to 200 mV shown in Fig. 8 varies from 20 to 100%, which is in good agreement with the experimental data of Fig. 7. This implies that ordinary barrier transmission can explain the overall change of the background conductance of these Nb-Au point-contact junctions.

This result for low-barrier-height junctions, that high-resistance junctions (thicker barriers) display a strongly increasing $\sigma(V)$, whereas low-resistance junctions (thinner barriers) will have a weak dependence, is general. It has also been observed in junctions with In-oxide barriers[22] for which the barrier height ~40 meV.

The Nb data give insight into how the background conductance in HTS might change as the junction resistance is lowered. There is increasing evidence that the surface layers of HTS, which serve as tunnel barriers, have low-barrier potentials.[23] In previous models,[11,12] there is a competition between the barrier effect, which is an increasing function of bias voltage, and the $N_n(E)$ effect which is a decreasing function of voltage. For low-resistance Nb junctions [Fig. 7(a)], the background conductance is relatively flat and, with a similar barrier effect in HTS, we would expect the $N_n(E)$ term to dominate giving an overall decreasing background conductance. High-resistance Nb junctions [Fig. 7(b)] have a much stronger barrier effect and, if a similar barrier term was found in high-resistance junctions on HTS, then it would likely dominate the $N_n(E)$ term, giving an overall increasing background conductance. Thus, our investigation of Nb-oxide barriers has provided a possible explanation for the changing background behavior found in HTS crystals.[11,12]

IV. CONCLUSIONS

To our knowledge, this is the first demonstration that the point-contact tunneling technique can perform phonon spectroscopy on a moderately coupled superconductor such as Nb. We emphasize that the measured signal represents a change of conductance of about 1% in the energy range corresponding to peaks in $F(\omega)$, requiring a conductance which is stable to a few parts in 10^3. Considering the relatively high junction resistances in the point-contact geometry compared to thin-film junctions and the potential for mechanical instabilities, it was gratifying to demonstrate that the point-contact technique could meet the requirements for noise and stability. The location and magnitude of the phonon structures we observe are in good agreement with other published studies of Nb using thin-film junctions. In particular, we consistently see the subtle low-energy phonon structure at 10 meV, which had previously been observed only for thin-film junctions on the (100) face of Nb single crystals. The observation of such subtle phonon structures in Nb indicates that the point-contact tunneling method does not necessarily introduce structural artifacts into the dynamic conductance and therefore can be considered a viable technique for the search of phonon effects or other mechanisms in HTS.

We have also demonstrated that the high-bias tunneling conductance displays the characteristic background behavior typical of barrier transmission. In this case, the barrier is Nb oxide, which has a relatively low potential height of about 250 meV. The high-bias behavior of the Nb junctions has given an important insight into the barrier effect on the background conductance when the applied voltage is on the order of the barrier height. This is relevant to the study of HTS, as it is becoming increasingly apparent that the natural surface layers of these materials exhibit barriers with relatively low barrier heights.[23] In particular, point-contact Nb junctions with widely varying resistances never displayed the anomalous decrease of the background conductance with voltage that are observed in point-contact junctions on[11] Bi-Pb-Sr-Ca-Cu-O and[12] Tl-Ba-Ca-Cu-O. A simple model for heating, applied to the HTS measurements, puts limits on the minimum junction radius which would be required to explain the decreasing background conductance.[11,12]

ACKNOWLEDGMENTS

The authors would like to thank Josh Stein for assitance with the data acquisition system. The work was supported by the U.S. Department of Energy, Division

of Basic Energy Sciences–Materials Sciences under Contract No. W-31-109-ENG-38 and the National Science Foundation–Office of Science and Technology Centers under Contract No. STC-8809854 (Q.H. and J.F.Z. Science and Technology Center for Superconductivity, University of Illinois–Urbana-Champaign). Q.H. acknowledges support from the Division of Educational Programs, Argonne National Laboratory.

---

*Also at Illinois Institute of Technology, Chicago, Illinois 60616.

[1]E. L. Wolf, *Principles of Electron Tunneling Spectroscopy* (Oxford University Press, New York, 1985).

[2]G. Binnig and H. Rohrer, IBM J. Res. Dev. **30**, 355 (1985).

[3]A. L. de Lozanne, S. A. Elrod, and C. F. Quate, Phys. Rev. Lett. **54**, 2433 (1985).

[4]H. G. Le Duc, W. J, Kaiser, and J. A. Stern, Appl. Phys. Lett. **50**, 1921 (1987).

[5]H. F. Hess, R. B. Robinson, R. C. Dynes, J. M. Valles, Jr., and J. V. Waszcak, Phys. Rev. Lett. **62**, 214 (1989); H. F. Hess, R. B. Robinson, and J. V. Waszczak, *ibid.* **64**, 2711 (1990).

[6]K. E. Gray, Mod. Phys. Lett. B **2**, 1125 (1988).

[7]P. J. M. van Bentum, R. T. M. Smokers, and H. van Kempen, Phys. Rev. Lett. **60**, 2543 (1988).

[8]K. Mullen, E. Ben-Jacob, and S. Ruggiero, Phys. Rev. B **38**, 5150 (1988).

[9]J. R. Kirtley and D. J. Scalapino, Phys. Rev. Lett. **65**, 798 (1990).

[10]M. E. Hawley, K. E. Gray, B. D. Terris, H. H. Wang, K. D. Carlson, and J. M. Williams, Phys. Rev. Lett. **57**, 629 (1986).

[11]Qiang Huang, J. F. Zasadzinski, K. E. Gray, J. Z. Liu, and H. Claus, Phys. Rev. B **40**, 9366 (1989).

[12]Qiang Huang, J. F. Zasadzinski, K. E. Gray, E. D. Bukowski, and D. M. Ginsberg, Physica C **161**, 141 (1989).

[13]E. L. Wolf, J. Zasadzinski, J. W. Osmun, and G. B. Arnold, J. Low Temp. Phys. **40**, 19 (1980).

[14]Z. G. Khim, D. M. Burnell, and E. L. Wolf, Solid State Commun. **39**, 159 (1981).

[15]J. Geerk, M. Gurvitch, D. B. McWhan, and J. M. Rowell, Physica B+C **109&110**, 1775 (1982).

[16]E. L. Wolf, T. P. Chen, and D. M. Burnell, Phys. Rev. B **31**, 6096 (1985).

[17]S. M. Durbin, D. S. Buchanan, J. E. Cunningham, and D. M. Ginsberg, Phys. Rev. B **28**, 6277 (1983).

[18]Ragnar Holm, J. Appl. Phys. **22**, 569 (1951).

[19]J. M. Rowell, M. Gurvitch, and J. Geerk, Phys. Rev. B **24**, 2278 (1981).

[20]A. A. Lysykh, A. M. Duif, A. G. M. Jansen, P. Wyder, and A. de Visser, Phys. Rev. B **38**, 1067 (1988).

[21]S. J. Hagen, Z. Z. Wang, and N. P. Ong, Phys. Rev. B **40**, 9389 (1989).

[22]Q. Huang, J. Zasadzinski, and K. E. Gray (unpublished).

[23]J. R. Kirtley, Inter. J. Mod. Phys. B **4**, 201 (1990).